Mitochondrial regulation by c-Myc and hypoxia-inducible factor-1α controls sensitivity to econazole

Yongmao Yu,[1] Maryam Niapour,[1] Yicheng Zhang,[3] and Stuart A. Berger[1,2]

[1]Arthritis and Immune Disorder Research Centre, University Health Network and [2]Department of Immunology, University of Toronto, Toronto, Ontario, Canada and [3]Department of Hematology, Tongji Hospital, Tongji Medical College, and Huazhong University of Science and Technology, Wuhan, China

Abstract

Econazole is an azole antifungal with anticancer activity that blocks Ca^{2+} influx and stimulates endoplasmic reticulum (ER) Ca^{2+} release through the generation of mitochondrial reactive oxygen species (ROS), resulting in sustained depletion of ER Ca^{2+} stores, protein synthesis inhibition, and cell death. c-Myc, a commonly activated oncogene, also promotes apoptosis in response to growth factor withdrawal and a variety of chemotherapeutic agents. We have investigated the role of c-myc in regulating sensitivity to econazole. Here, we show that c-myc-negative cells are profoundly resistant to econazole. c-Myc-negative rat fibroblasts failed to generate mitochondrial ROS in response to econazole and consequently failed to deplete the ER of Ca^{2+}. HL60 cells knocked down for c-myc expression also displayed decreased ROS generation and decreased econazole sensitivity. Addition of H_2O_2 restored sensitivity to econazole in both c-myc-negative rat fibroblasts and c-myc knocked-down HL60 cells, supporting a role for ROS in cell death induction. c-Myc-negative cells and HL60 cells knocked down for c-myc have reduced mitochondrial content compared with c-myc-positive cells. The hypoxia sensor, hypoxia-inducible factor-1α (HIF-1α), interacts antagonistically with c-myc and also regulates mitochondrial biogenesis. Knockdown of HIF-1α in c-myc-negative cells increased mitochondrial content restored ROS generation in response to econazole and increased sensitivity to the drug. Taken together, these results show that c-myc and HIF-1α

regulate sensitivity to econazole by modulating the ability of the drug to generate mitochondrial ROS. [Mol Cancer Ther 2008;7(3):483–91]

Introduction

The endoplasmic reticulum (ER) is a key organelle responsible for the synthesis and post-translational processing of proteins destined for secretion or the cell surface (1, 2). The ER is also a major repository for intracellular Ca^{2+} and plays a central role in regulating Ca^{2+} transients (3). Disruption of Ca^{2+} stores in the ER, such as with the sarcoplasmic/ER Ca^{2+} ATPase (SERCA) inhibitor thapsigargin (4), can lead to ER stress and cell death (5, 6). Previously, we and others described induction of ER stress by the imidazole antifungal econazole (7–14). This agent disrupts ER Ca^{2+} stores by both promoting ER Ca^{2+} release and blocking Ca^{2+} influx (9, 10, 12, 15–19). The result is sustained depletion of ER Ca^{2+} stores, inhibition of protein synthesis, and cell death. Work to date indicates that econazole has promise as an anticancer agent due to its unique mechanism of action, relative insensitivity to drug resistance mechanisms, and great differential sensitivity of tumor cells to the drug (8, 9, 11, 20).

Although much is now known about how econazole induces ER stress, little is known with respect to cellular and genetic factors regulating sensitivity. Previously, we generated and characterized variants of the human myelomonocytic leukemia cell line HL60 that exhibited decreased sensitivity to econazole (12). Although these lines were selected for resistance to econazole, they also exhibited resistance to other ER stress agents including thapsigargin, tunicamycin, and DTT, thus identifying a multidrug resistance phenotype associated specifically with ER stress. Furthermore, these clones exhibited increased Ca^{2+} influx and increased ribosomal protein content, consistent with Ca^{2+} stores and protein synthesis as important targets for econazole-induced cell death.

A variety of tumor cells has been observed to be sensitive to econazole. For example, we showed that acute myelogenous leukemia blast cells obtained from patients exhibited 3.7 to 4.6 logs greater sensitivity to econazole than normal human hemopoietic progenitor cells (9). Human breast cancer cells exhibited 2.5 to 3 logs reduction in clonogenicity under conditions that resulted in only 0.2 log reduction in normal cells (11). Furthermore, the sensitivity of breast cancer cells to econazole could be enhanced 10-fold by concurrently stimulating them with epidermal growth factor or bombesin. Other groups have shown that prostate cancer cells (14) and colon cancer cells (13) are also sensitive to econazole. However, genetic or other factors associated with tumor cells that might regulate sensitivity to econazole have not yet been identified.

One common oncogene associated with a variety of human tumors is c-myc. c-Myc is a transcription factor that regulates, in partnership with its binding partner max, upwards of 15% of all human genes (21). Many c-myc target genes are involved in protein synthesis, cell cycle, cell growth and size, and metabolism in both normal and abnormal cells. c-myc dysregulation has been implicated in as many as 60% of all human tumors (22) either through overexpression, translocation, or mutation (23, 24). Whereas c-myc overexpression stimulates cell growth, paradoxically, c-myc dysregulation can also promote apoptosis in response to growth factor withdrawal and a variety of chemotherapeutic agents (22, 25, 26). A previous report showed that rat-1 cells over-expressing c-myc displayed increased sensitivity to the ER stress agents thapsigargin and tunicamycin (27). Because c-myc regulates cellular functions associated with ER stress such as protein synthesis and also enhances sensitivity to known ER stress agents, we therefore investigated the role of c-myc in regulating sensitivity to econazole.

Materials and Methods

Cells and Cell Culture

Human HL60 promyelocytic leukemia cells were grown in RPMI 1640 containing 10% fetal bovine serum (FBS) and antibiotics. c-Myc-negative rat-1-derived HO15.19 cells (c-myc-negative) and HO15.19 cells expressing c-myc (c-myc-positive; ref. 28) were a kind gift from Dr. Linda Penn (Ontario Cancer Institute) and were grown in DMEM containing 10% FBS in tissue culture flasks T75 (Sarstedt).

Apoptosis

To measure apoptosis induced by econazole, cells were treated with econazole in RPMI containing 1% FBS for 2 h at 37°C then further incubated overnight in RPMI containing 10% FBS. For other ER stress-inducing agents, cells were treated with thapsigargin or tunicamycin in RPMI containing 5% FBS. The cells were washed with PBS and stained with Annexin V-Cy5 Apoptosis Detection kit (Biovision)/propidium iodide and analyzed by flow cytometry. Econazole, thapsigargin, and tunicamycin were obtained from Sigma.

Western Blot

Cells were washed with cold PBS and lysed with lysis buffer [1.5 mL of 10% SDS, 1.5 mL glycerol, 1.2 mL of 1 mol/L Tris (pH 6.8), 9.3 mL double-distilled H_2O]. DNA was sheared with a 22-gauge needle and kept on ice for 20 min. The lysate was boiled for 8 min and centrifuged at $14,000 \times g$ for 20 min at 4°C. Protein concentration of the supernatant was determined with BCA Protein Assay Reagent kit (Pierce). Protein (40 μg) was mixed with 1:10 volume of fresh β-mercaptoethanol and 1:100 volume of bromophenol blue [1% in 1 mol/L Tris-HCl (pH 6.8)], boiled for 4 min, and loaded onto 10% SDS-PAGE. The proteins were transferred onto Immobilon-P membranes (Millipore) and blotted with c-myc Ab-5 (clone 67P05) antibody (Labvision/Neomarker). Mouse actin (pan Ab-5;

clone ACTN05) (Labvision/Neomarker) was used as a loading control.

Small Interfering RNA

HO15.19 cells were incubated in DMEM H-21 supplemented with 10% FBS at 37°C in a humidified 5% CO_2 incubator. Transfection of small interfering RNA was carried out by using HiPerFect transfection reagent (Qiagen) as described by the manufacturer. The sequence for rat hypoxia-inducible factor-1α (HIF-1α) was designed using the Qiagen online siRNA design tool and was 5′GCGGCGAGAACGAGAAGAAAA3′.

Construction of Lentivirus Vectors

The empty lentivirus vector pLEN (H1GFP), in which the H1 promoter drives expression of short hairpin RNA sequences (29), was a gift from Dr. John Dick (University Health Network). The sequences of the oligos used were human c-myc 1330: 5′-TAAGATGAGGAAGAAATC-GATGTGGATCCACATCGATTTCTTCCTCATCTTTTT-3′ and 5′-CTAGAAAAAGATGAGGAAGAAATCGATGTGG-ATCCACATCGATTTCTTCCTCATCTTAAT-3′ and human c-myc 917: 5′-TAAACGACGAGACCTTCATCAAAG-GATCCTTTGATGAAGGTCTCGTCGTTTTTT-3′ and 5′-CTAGAAAAAACGACGAGACCTTCATCAAAG-GATCCTTTGATGAAGGTCTCGTCGTTTAAT-3′. Each pair of oligos was mixed and annealed by incubating at 95°C for 5 min and was cooled slowly. The annealed mixture (1 μL) was ligated into pLEN vector that had been digested with *Pac*I and *Xba*I.

Generation of the Infective Lentivirus

Lentivirus vectors harboring human c-Myc short hairpin RNA were produced by transient transfection into 293T cells as described previously (30). Briefly, the backbone plasmid vector construct (10 μg) was mixed with the accessory plasmids VSVG (3.5 μg), pRRE (6.5 μg), and pREV (2.5 μg) and transfected into 293T cells with the Calphos Mammalian Transfection Kit (Clontech). The cell supernatant was replaced with 4 mL fresh Iscove's MEM (10% FCS) at 24 h and virus was harvested at 48 h after the plasmid transfection.

Lentiviral Infection

A total of 0.1×10^6 HL60 cells were infected with 2 mL lentivirus culture supernatant ($\sim 2 \times 10^6$ virus particles) in the presence of 8 μg/mL polybrene (Sigma-Aldrich) for 4 days. Green fluorescent protein–positive cells were sorted by fluorescence-activated cell sorting and grown in RPMI (10% FBS) for further analysis.

Ca^{2+} Measurement

$[Ca^{2+}]_c$ measurements were done by flow cytometry. Cells (5×10^5/mL) were serum deprived for ~ 2 h in Tyrode's buffer (10 mmol/L HEPES, 100 mmol/L NaCl, 5 mmol/L KCl, 1.4 mmol/L $CaCl_2$, 1 mmol/L $MgCl_2$, 5.6 mmol/L glucose, 0.05% bovine serum albumin). Cells were then incubated in indo-1 loading buffer (30 min, 37°C; 5 μmol/L indo-1AM, 0.03% pluronic F-127 in Tyrode's buffer), washed (two times), and incubated at room temperature (>15 min) to allow for the complete removal and/or conversion of indo-1AM to Ca^{2+}-sensitive indo-1. Measurements were done using a laser tuned to 338 nm

while monitoring emissions at 405 and 450 nm. The concentration of intracellular free Ca^{2+} was calculated according to the following formula (Grynkiewcz, 1985):

$$[Ca^{2+}]_i = K_d \times (F_{min}/F_{max}) \times (R - R_{min})/(R_{max} - R),$$

where R is the ratio of the fluorescence intensities measured at 405 and 450 nm during the experiments and F is the fluorescence intensity measured at 450 nm. R_{min}, R_{max}, F_{min}, and F_{max} were determined from *in situ* calibration of unlysed cells using 4 μmol/L ionomycin in the absence (R_{min} and F_{min}; 10 mmol/L EGTA) and presence of (R_{max} and F_{max}) of Ca^{2+}. K_d (250 nmol/L) is the dissociation constant for indo-1 at 37°C. R_{min}, R_{max}, F_{min}, and F_{max} varied depending on settings and were determined at the beginning of each experimental procedure.

Reactive Oxygen Species Generation

To determine mitochondrial reactive oxygen species (ROS) generation in response to econazole in real time, 0.5×10^6 cells were incubated with 5 μmol/L MitoSOX Red (Molecular Probes) for 8 min at 37°C. The cells were cooled down at room temperature for 2 min and fluorescence was measured over time by flow cytometry using the LSRII (Becton Dickinson). Econazole (15 μmol/L) or same volume of carrier (DMSO) was added at the 30-s time interval and data were recorded for 10 min. FlowJo (TreeStar) was used to analyze the data. In other experiments, to determine the ROS level changes to drugs at different time points, 0.5×10^6 cells in triplicates were stained with 5 μmol/L MitoSOX Red for 10 min at 37°C and put on ice. Mean fluorescence intensity of the dye staining was determined using FACSCalibur or LSRII flow cytometer (Becton Dickinson).

Mitochondrial Mass

To measure mitochondrial content, 0.5×10^6 cells in triplicates were put into AFCS tubes and stained with 200 nmol/L MitoTracker Deep Red 633 (Molecular Probes). The cells were incubated at 37°C for 15 min then put on ice. Mean fluorescence intensity of the dye staining was determined with the FACSCalibur flow cytometer (Becton Dickinson).

Electron Microscopy

Approximately 1×10^6 cells were pelleted and fixed in 2% gluteraldehyde in 0.1 mol/L cacodylate buffer (pH 7.3) for 2 h. The fixed samples were washed, stained with 1% osmium tetroxide for 90 min, dehydrated with a graded series of ethanol, and transitioned with propylene oxide to Spurr resin. After overnight incubation, the samples were placed in embedding molds and polymerized over night at 65°C. Samples were sectioned and imaged with a Tecnai 20 transmission electron microscope (FEI Company). High-resolution TIFF images were analyzed for cytoplasmic and mitochondrial content using ImageJ (NIH).
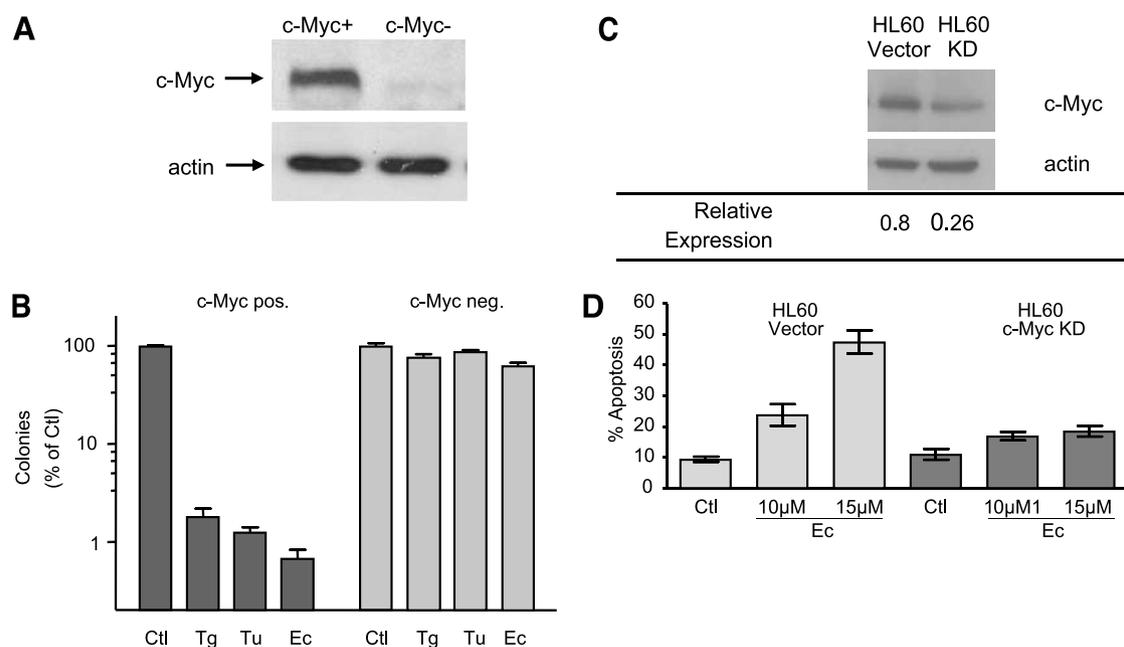

Figure 1. c-Myc-negative and c-myc knocked-down cells are resistant to econazole. **A,** Western blot of c-myc expression in rat-1 fibroblast cells deleted for c-myc and with reconstituted c-myc. **B,** rat-1 cells expressing c-myc and rat-1 cells deleted for c-myc were exposed to ER stress agents thapsigargin (100 nmol/L), tunicamycin (200 ng/mL), or econazole (12 μmol/L) overnight. Cells were collected and transferred to fresh plates at lower dilution to assay for colony-forming ability. *Bars,* SE of duplicate independent measurements. Representative of three independent experiments. **C,** HL60 cells were coinfected with two lentiviral short hairpin RNA constructs targeting separate regions of c-myc (917 and 1,330; GenBank accession no. V00568). Cells were sorted for green fluorescent protein expression and c-myc expression was evaluated by Western blot. Relative expression refers to normalized expression relative to actin. Knockdown efficiency is ~67%. **D,** HL60 cells were exposed to 10 or 15 μmol/L econazole overnight. % Apoptosis was determined by Annexin V staining as described in Materials and Methods. Averages of duplicate independent measurements. Representative of at least four independent lentiviral infections.

Results

c-Myc Regulation of Sensitivity to Econazole

McCullough et al. showed that rat-1 cells overexpressing c-myc exhibited increased sensitivity to the ER stress agents thapsigargin and tunicamycin (27). To investigate the possibility that c-myc also regulates sensitivity to econazole, we exposed c-myc-negative and c-myc-positive rat-1 cells (Fig. 1A) to econazole. The cells were then collected and replated at lower dilution to allow discrete colonies to form from the surviving cells. As shown in Fig. 1B, c-myc-expressing cells exhibited sensitivity to thapsigargin, tunicamycin, and econazole. In contrast, we observed that c-myc-negative cells were almost completely resistant to the ER stress agents. These results therefore confirm the results of McCullough et al. and show that the absence of c-myc also renders these cells resistant to econazole.

c-Myc Knockdown Reduces Sensitivity to Econazole

To further confirm a role for c-myc in regulating sensitivity to econazole, we knocked down expression of c-myc in human myelomonocytic leukemia HL60 cells using lentiviral-mediated short hairpin RNA and tested sensitivity to econazole. Cells were infected with the virus and then sorted using the green fluorescent protein fluorescent marker by fluorescence-activated cell sorting. As shown in Fig. 1C, lentiviral infection resulted in a decrease of c-myc expression by 67% compared with vector control. It is of interest to note that HL60 cells knocked down for c-myc displayed decreased growth rate and, after several weeks in culture, lost both green fluorescent protein expression and the c-myc knockdown effect. This likely reflects the dependence on c-myc for growth of these cells. Nevertheless, the knockdown effect was sustained for several weeks following sorting, allowing us to test sensitivity. As shown in Fig. 1D, when the cells were exposed to econazole, the c-myc knocked-down cells displayed a reduced level of apoptosis compared with vector control-infected cells. These results therefore support a role for c-myc in regulating sensitivity to econazole.

Impaired ER Ca²⁺ Release in c-myc-Negative Cells

We showed previously that econazole induces ER stress by depleting the ER of Ca^{2+} (10, 12). The depletion occurs through the combination of direct stimulation of ER Ca^{2+} release combined with blocking Ca^{2+} influx at the membrane. To investigate whether c-myc affected either of these properties, we measured Ca^{2+} release in both c-myc positive and c-myc-negative cells in response to either thapsigargin or econazole. As shown in Fig. 2A, exposure of c-myc-negative or c-myc-positive cells to thapsigargin resulted in a large increase in cytoplasmic Ca^{2+}. This transient elevation was due to both influx and mobilization as shown by the decreased Ca^{2+} transient observed in the presence of the nonspecific Ca^{2+} influx blocking agent Ni^{2+} (Fig. 2B). In either case, however, no significant differences in the magnitude of thapsigargin-stimulated Ca^{2+} signals were observed between c-myc-positive and c-myc-negative cells. As shown in Fig. 2C, exposure of c-myc positive cells to econazole resulted in increased cytoplasmic Ca^{2+},
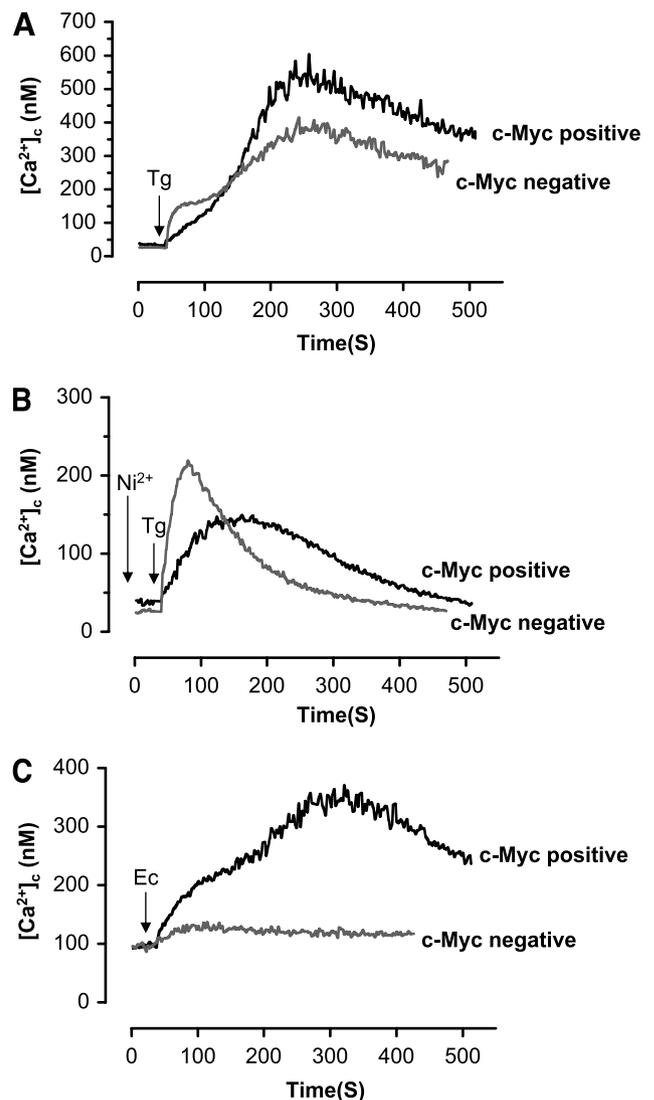

Figure 2. c-myc-negative cells fail to mobilize Ca^{2+} from the ER. c-myc-negative and c-myc-positive rat fibroblasts were collected and loaded with indo-1 as described in Material and Methods. Cytoplasmic Ca^{2+} levels were monitored by flow cytometry following addition of (**A**) thapsigargin (3 μmol/L), (**B**) thapsigargin plus Ni^{2+} (5 mmol/L), or (**C**) 15 μmol/L econazole. Representative of two independent experiments.

reflecting ER Ca^{2+} mobilization. In contrast, exposure of c-myc-negative cells to econazole failed to stimulate significant Ca^{2+} mobilization. Therefore, whereas both c-myc-negative and c-myc-positive cells released similar levels of Ca^{2+} from the ER in response to thapsigargin and displayed similar levels of influx, econazole failed to stimulate ER Ca^{2+} release from c-myc-negative cells.

Decreased Mitochondrial ROS Generation by Econazole in c-myc-Negative Cells

We showed previously that the ability of econazole to stimulate ER Ca^{2+} release was dependent on the generation of ROS at the mitochondria (19). This property of econazole was observed to be dependent on complex III of

the electron transport chain as it could be suppressed by intracellular antioxidants and the complex III inhibitor antimycin A. Our observation that econazole failed to deplete the ER of Ca^{2+} in c-myc-negative cells suggested to us that this might be due to a failure to generate ROS. To investigate this possibility, we measured ROS generation in mitochondria in response to econazole. As shown in Fig. 3A, addition of econazole to c-myc-positive cells resulted in the immediate generation of mitochondrial ROS. In contrast, exposure of c-myc-negative cells to econazole did not generate ROS. These observations suggest that econazole fails to deplete the ER in c-myc-negative cells due to an inability to generate mitochondrial ROS.

c-Myc Knockdown Reduces ROS Generation by Econazole

To further confirm a role for c-myc in regulation of econazole-induced ROS, we tested mitochondrial ROS generation in HL60 cells knocked down for c-myc. As shown in Fig. 3B, HL60 cells knocked down for c-myc generated significantly less ROS than control HL60 cells. This observation is therefore consistent with a role for c-myc in regulating ROS generation at the mitochondria.

H_2O_2 Restores Sensitivity to Econazole in c-myc-Negative and c-myc Knocked-Down Cells

To further explore the functional importance of ROS generation, we added back H_2O_2 to cells exposed to econazole. As shown in Fig. 3C, H_2O_2 on its own had little toxic effect on c-myc-negative cells. However, when added with econazole, c-myc-negative cells underwent apoptosis to a greater extent than that of econazole or H_2O_2 alone. Furthermore, H_2O_2 slightly enhanced the sensitivity of c-myc-overexpressing cells to econazole. As shown in Fig. 3D, we observed a similar effect in HL60 cells knocked down for c-myc. The observation that H_2O_2 can restore sensitivity to econazole in c-myc-negative or c-myc knocked-down cells supports the model that c-myc regulates sensitivity to econazole by controlling its ability to generate ROS.

c-Myc Regulation of Mitochondrial Content

Li et al. showed previously that c-myc could regulate mitochondrial biogenesis (31). Our observation that c-myc-negative cells failed to generate mitochondrial ROS in response to econazole suggested that this could be related to decreased mitochondrial content. We therefore investigated mitochondrial content using two methods. First, we stained cells with MitoTracker Red, a mitochondria-specific dye, and measured content by flow cytometry. As shown in Fig. 4A and B, c-myc-negative cells had significantly decreased mitochondrial content compared with c-myc-positive cells. We further observed a similar decrease in mitochondrial content in HL60 cells knocked down for c-myc expression (Fig. 4C). To further confirm this observation, we performed morphometric analysis on electron micrographs of cells, measuring mitochondrial
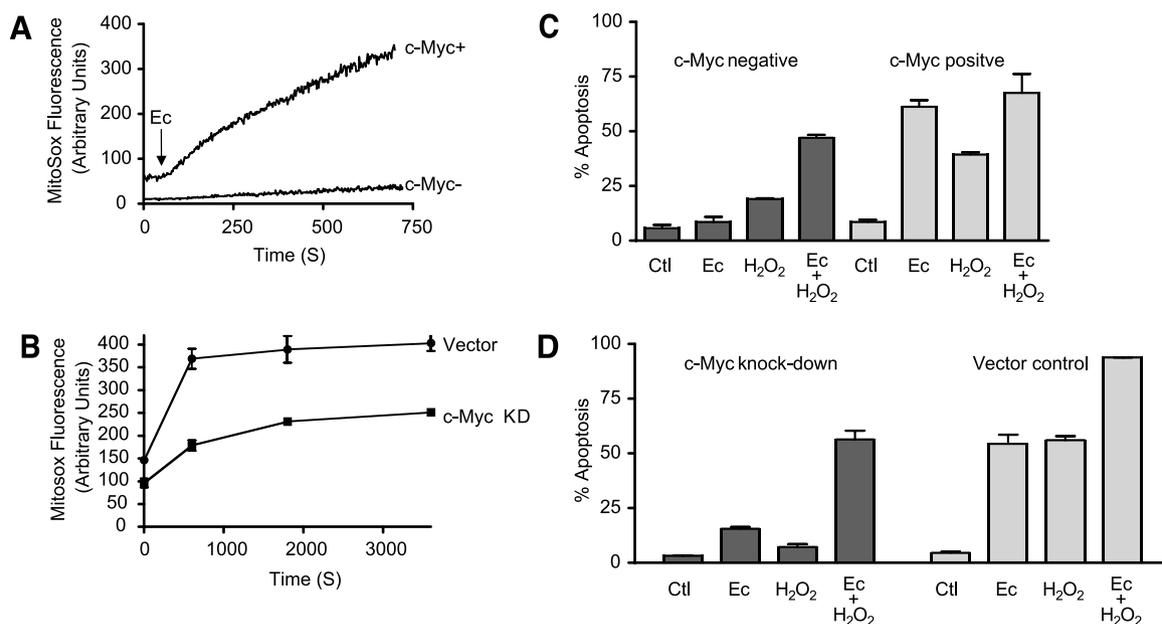

Figure 3. Failure to generate ROS in response to econazole and restoration of sensitivity to econazole with H_2O_2 in c-myc-negative or knocked-down cells. c-myc-positive or c-myc-negative rat-1 cells were labeled with the mitochondrial ROS-sensitive dye MitoSOX Red. Econazole (15 μmol/L) was added and fluorescence was followed over time. **A,** c-myc-negative and c-myc-positive rat fibroblasts. **B,** c-myc knocked-down and vector control HL60 cells. Econazole (15 μmol/L) was added, the cells were incubated for the indicated periods, and fluorescence intensity was measured by flow cytometry. *Points,* average of measurements; *bars,* SE. Both experiments were repeated at least twice with similar results. **C,** c-myc-negative or c-myc-positive cells were exposed to econazole (10 μmol/L), H_2O_2 (0.5 μmol/L), or both agents overnight. The cells were then collected and assayed for apoptotic cells by flow cytometry. **D,** HL60 cells knocked down for c-myc or vector control cells were exposed to econazole (10 μmol/L), H_2O_2 (0.5 μmol/L), or both agents overnight. The cells were then collected and assayed for apoptotic cells by flow cytometry. *Bars,* SE of duplicate independent measurements. Both experiments were repeated twice with similar results.
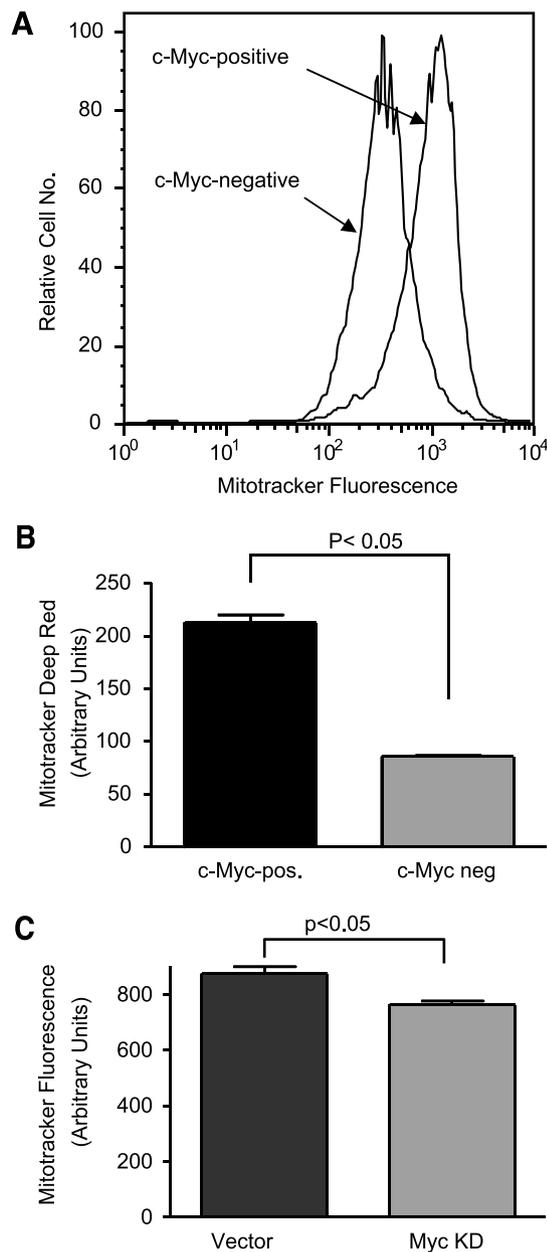
A

B

C

Figure 4. Reduced mitochondrial content in c-myc-negative or knocked-down cells. c-myc-negative or c-myc-positive rat fibroblasts were labeled with MitoTracker Red and analyzed by flow cytometry. **A,** histogram of MitoTracker Red staining. **B,** mean fluorescence (average of three measurements). **C,** histogram of MitoTracker Red–stained HL60 c-myc knocked-down or vector control cells.

area as a proportion of total cellular area. As summarized in Table 1, c-myc-negative cells were observed to have decreased mitochondrial content compared with myc-positive cells in proportion to that observed with MitoTracker Red staining. These observations therefore confirm that c-myc expression influences mitochondrial content.

HIF-1α Knockdown Restores Mitochondrial Content, ROS Generation, and Econazole Sensitivity in c-myc-Negative Cells

Our previous work showed that ROS generation by econazole was dependent on complex III of the electron transport chain (19). Recently, Bell et al. showed that complex III was also required for generating the ROS that stabilizes HIF-1α, the hypoxia sensor that regulates the balance between aerobic and anaerobic metabolism (32). HIF-1α has also been shown to interact in an antagonistic fashion with c-myc and regulate mitochondrial biogenesis (33). Given our observations of decreased mitochondrial content and decreased ROS production by econazole in c-myc-negative cells, we investigated a possible role for HIF-1α in mediating resistance to econazole. We knocked down HIF-1α using small interfering RNA in c-myc-negative cells. As shown in Fig. 5A, HIF-1α was knocked down by ~60% when normalized for actin expression. As shown in Fig. 5B, decreased HIF-1α levels resulted in increased mitochondrial content, restoration of ROS generation in response to econazole (Fig. 5C), and increased sensitivity to the drug (Fig. 5D). These results suggest that, in the absence of c-myc, HIF-1α is an important regulator of mitochondrial content, function, and sensitivity to econazole.

Discussion

c-Myc promotes cellular transformation and also increases cellular susceptibility to apoptosis. Here, we have shown that c-myc regulates sensitivity to the ER stress-inducing drug econazole. We showed that c-myc-negative cells were almost completely resistant to econazole and knockdown of c-myc in HL60 cells reduced econazole-induced apoptosis. Although c-myc-negative cells contained similar levels of Ca^{2+} in their ER, econazole failed to mobilize ER Ca^{2+} in these cells. We showed that this defect could be traced to an inability to generate mitochondrial ROS, an activity that we showed previously was required for econazole to deplete ER Ca^{2+} (19). We also showed that knocking down HIF-1α in c-myc-negative cells could restore mitochondrial content, ROS generation, and sensitivity to econazole, suggesting that HIF-1α is also a major regulator of econazole sensitivity. Taken together, these observations suggest that econazole targets c-myc-expressing cells through up-regulation of mitochondrial content and function by c-myc.

As observed previously (27) and confirmed in this study, c-myc controls sensitivity to thapsigargin. Thapsigargin acts by inhibiting the ATPase responsible for pumping Ca^{2+} into the ER against the Ca^{2+} gradient (34). When cells are exposed to thapsigargin, inhibition of the pump causes a rapid release of ER Ca^{2+}. ER Ca^{2+} depletion also stimulates Ca^{2+} influx, resulting in the large increase in cytoplasmic Ca^{2+} such as was observed in Fig. 2A. The mechanism by which c-myc affects sensitivity to thapsigargin is unknown; however, Barsyte-Lovejoy et al. documented that c-myc repressed ER stress genes in

Table 1. Decreased mitochondrial content in c-myc-negative cells

	No. electron microscopy images analyzed	No. mitochondria counted	Total cytoplasmic area (pixels)	Total mitochondrial area (pixels)	% Area mitochondrial/ cytoplasmic
c-myc negative	20	140	16,332,689	378,575	2.3
c-myc positive	12	113	7,952,376	6,023,04	7.40

NOTE: c-myc-negative and c-myc-positive rat fibroblasts were processed as described in Materials and Methods and imaged by electron microscopy. Images were analyzed morphometrically for cytoplasmic and mitochondrial content.

response to thapsigargin (35). However, our observation that c-myc status does not affect ER Ca^{2+} content or release by thapsigargin suggests that ER Ca^{2+} stores are unlikely to be the sole target. One consequence of the large Ca^{2+} signal stimulated by thapsigargin is Ca^{2+} loading of mitochondria (10, 36–38). In this circumstance, mitochondria act as buffers mitigating the large rise in cytoplasmic Ca^{2+}. However, if the mitochondrial Ca^{2+} increase is excessive, then an apoptotic response is triggered. This model suggests that mitochondria might be the critical target for thapsigargin-induced cell death.

The fact that c-myc affects mitochondrial status suggests that thapsigargin sensitivity may be controlled through mitochondrial function. This possibility remains to be investigated.

Although loss of c-myc decreased mitochondrial content, the loss was not absolute. However, the inability of c-myc-negative cells to generate ROS in response to econazole suggests an effect greater than would be expected based on mitochondrial loss. We showed previously that the ability of econazole to generate ROS was dependent on complex III activity (19). c-Myc
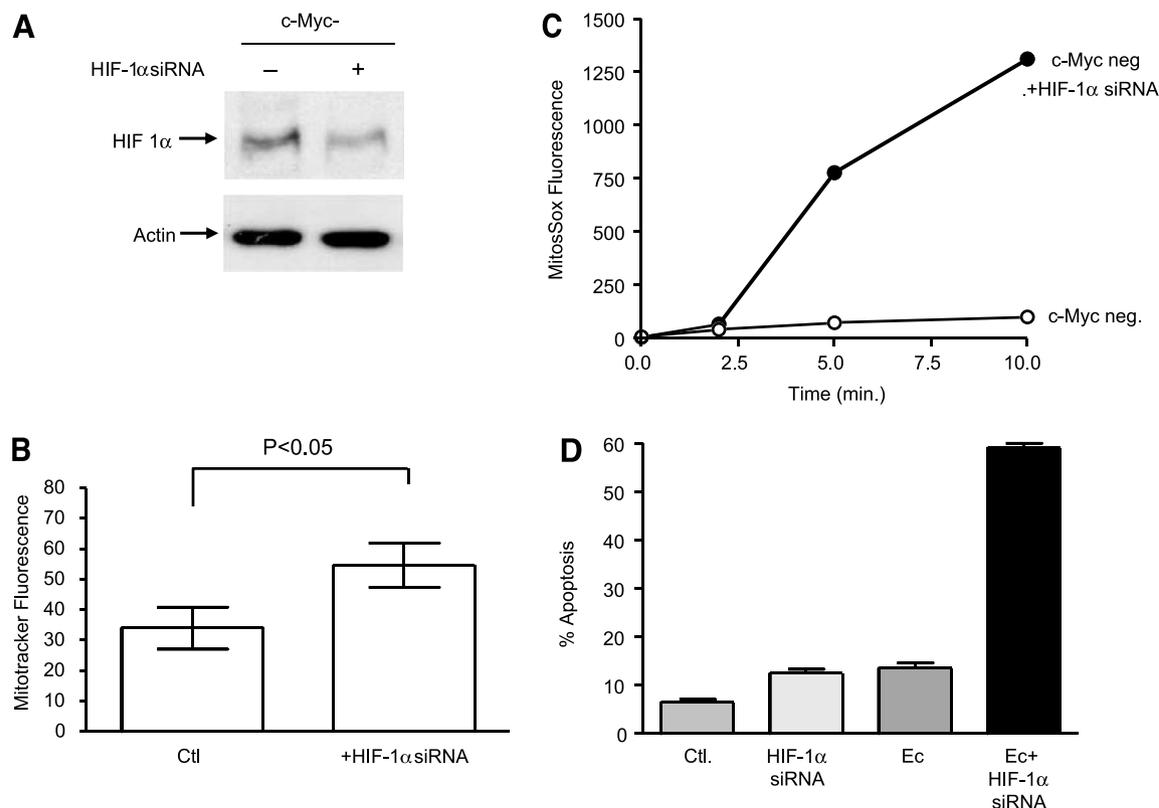

Figure 5. HIF-1α knockdown restores sensitivity to econazole. **A,** HIF-1α expression in c-myc-negative cells following knockdown. Protein reduction was ~60% as determined by densitometry and normalization to actin. **B,** cells were stained with MitoTracker Red as described in Materials and Methods and staining was measured by flow cytometry. Average of three independent measurements. **C,** control and HIF-1α knocked-down cells were labeled with MitoSOX Red and exposed to econazole for the indicated periods. Fluorescence was measured by flow cytometry. **D,** control or HIF-1α cells were incubated with econazole. The following day, % apoptosis was measured by Annexin V staining and flow cytometry. This experiment was repeated twice with similar results.

is known to regulate many genes involved in mitochondrial function. As summarized by Li et al. (31), at least 23 mitochondrial genes are bound by c-myc as determined by chromatin immunoprecipitation analysis. Li et al. also showed that c-myc regulates TFAM, a nuclearly encoded transcription factor that translocates to mitochondria and activates transcription. Therefore, it is possible that c-myc also regulates econazole-mediated ROS generation through its influence on mitochondrial genes.

Recently, Zhang et al. showed that HIF-1 could regulate mitochondrial biogenesis in renal carcinoma cells by antagonizing c-myc, both by activating expression of a myc transcriptional repressor and by promoting its degradation (33). Koshiji et al. also showed that HIF-1α could displace c-myc binding to the p21^{cip1} promoter, thereby inducing cell cycle arrest, as well as other myc targets (39). Our findings suggest that HIF-1α also plays another role of suppressing mitochondrial function in the absence of c-myc.

We and others have observed that tumor cells exhibit differential sensitivity to econazole. The observations described here suggest that an important factor regulating this effect may be mitochondrial regulation by c-myc. Furthermore, our finding that knockdown of HIF-1α restores sensitivity to econazole in the absence of c-myc suggests that appropriate targeting of this molecule *in vivo* may enhance the anticancer effectiveness of econazole.

References

1. Gorlach A, Klappa P, Kietzmann T. The endoplasmic reticulum: folding, calcium homeostasis, signaling, and redox control. Antioxid Redox Signal 2006;8:1391–418.

2. Zhang K, Kaufman RJ. Protein folding in the endoplasmic reticulum and the unfolded protein response. Handb Exp Pharmacol 2006;172:69–91.

3. Lewis RS. The molecular choreography of a store-operated calcium channel. Nature 2007;446:284–7.

4. Ali H, Christensen SB, Foreman JC, Pearce FL, Piotrowski W, Thastrup O. The ability of thapsigargin and thapsigargicin to activate cells involved in the inflammatory response. Br J Pharmacol 1985;85:705–12.

5. Ferri KF, Kroemer G. Organelle-specific initiation of cell death pathways. Nat Cell Biol 2001;3:E255–63.

6. Marciniak SJ, Ron D. Endoplasmic reticulum stress signaling in disease. Physiol Rev 2006;86:1133–49.

7. Najid A, Ratinaud MH. Comparative studies of steroidogenesis inhibitors (econazole, ketoconazole) on human breast cancer MCF-7 cell proliferation by growth experiments, thymidine incorporation and flow cytometric DNA analysis. Tumori 1991;77:385–90.

8. Gommerman JL, Berger SA. Protection from apoptosis by steel factor but not interleukin-3 is reversed through blockade of calcium influx. Blood 1998;91:1891–900.

9. Soboloff J, Zhang Y, Minden M, Berger SA. Sensitivity of myeloid leukemia cells to calcium influx blockade: application to bone marrow purging. Exp Hematol 2002;30:1219–26.

10. Soboloff J, Berger SA. Sustained ER Ca^{2+} depletion suppresses protein synthesis and induces activation-enhanced cell death in mast cells. J Biol Chem 2002;277:13812–20.

11. Zhang Y, Crump M, Berger SA. Purging of contaminating breast cancer cells from hematopoietic progenitor cell preparations using activation enhanced cell death. Breast Cancer Res Treat 2002;72:265–78.

12. Zhang Y, Berger SA. Increased calcium influx and ribosomal content correlate with resistance to endoplasmic reticulum stress-induced cell death in mutant leukemia cell lines. J Biol Chem 2004;279:6507–16.

13. Ho YS, Wu CH, Chou HM, et al. Molecular mechanisms of econazole-induced toxicity on human colon cancer cells: G$_0$-G$_1$ cell cycle arrest and caspase 8-independent apoptotic signaling pathways. Food Chem Toxicol 2005;43:1483–95.

14. Huang JK, Liu CS, Chou CT, et al. Effects of econazole on Ca^{2+} levels in and the growth of human prostate cancer PC3 cells. Clin Exp Pharmacol Physiol 2005;32:735–41.

15. Franzius D, Hoth M, Penner R. Non-specific effects of calcium entry antagonists in mast cells. Pflugers Arch 1994;428:433–8.

16. Gamberucci A, Fulceri R, Bygrave FL, Benedetti A. Unsaturated fatty acids mobilize intracellular calcium independent of IP3 generation and VIA insertion at the plasma membrane. Biochem Biophys Res Commun 1997;241:312–6.

17. Gamberucci A, Fulceri R, Benedetti A, Bygrave FL. On the mechanism of action of econazole, the capacitative calcium inflow blocker. Biochem Biophys Res Commun 1998;248:75–7.

18. Jan CR, Ho CM, Wu SN, Tseng CJ. Multiple effects of econazole on calcium signaling: depletion of thapsigargin-sensitive calcium store, activation of extracellular calcium influx, and inhibition of capacitative calcium entry. Biochim Biophys Acta 1999;1448:533–42.

19. Zhang Y, Soboloff J, Zhu Z, Berger SA. Inhibition of Ca^{2+} influx is required for mitochondrial reactive oxygen species-induced endoplasmic reticulum Ca^{2+} depletion and cell death in leukemia cells. Mol Pharmacol 2006;70:1424–34.

20. Cogswell S, Berger S, Waterhouse D, Bally MB, Wasan EK. A parenteral econazole formulation using a novel micelle-to-liposome transfer method: *in vitro* characterization and tumor growth delay in a breast cancer xenograft model. Pharm Res 2006;23:2575–85.

21. Dang CV, O'Donnell KA, Zeller KI, Nguyen T, Osthus RC, Li F. The c-Myc target gene network. Semin Cancer Biol 2006;16:253–64.

22. Vita M, Henriksson M. The Myc oncoprotein as a therapeutic target for human cancer. Semin Cancer Biol 2006;16:318–30.

23. Oster SK, Ho CS, Soucie EL, Penn LZ. The myc oncogene: marvelously complex. Adv Cancer Res 2002;84:81–154.

24. Meyer N, Kim SS, Penn LZ. The Oscar-worthy role of Myc in apoptosis. Semin Cancer Biol 2006;16:275–87.

25. Evan GI, Wyllie AH, Gilbert CS, et al. Induction of apoptosis in fibroblasts by c-myc protein. Cell 1992;69:119–28.

26. Gibson AW, Cheng T, Johnston RN. Apoptosis induced by c-myc overexpression is dependent on growth conditions. Exp Cell Res 1995;218:351–8.

27. McCullough KD, Martindale JL, Klotz LO, Aw TY, Holbrook NJ. Gadd153 sensitizes cells to endoplasmic reticulum stress by down-regulating Bcl2 and perturbing the cellular redox state. Mol Cell Biol 2001;21:1249–59.

28. Mateyak MK, Obaya AJ, Adachi S, Sedivy JM. Phenotypes of c-Myc-deficient rat fibroblasts isolated by targeted homologous recombination. Cell Growth Differ 1997;8:1039–48.

29. van de Wetering M, Oving I, Muncan V, et al. Specific inhibition of gene expression using a stably integrated, inducible small-interfering-RNA vector. EMBO Rep 2003;4:609–15.

30. Dull T, Zufferey R, Kelly M, et al. A third-generation lentivirus vector with a conditional packaging system. J Virol 1998;72:8463–71.

31. Li F, Wang Y, Zeller KI, et al. Myc stimulates nuclearly encoded mitochondrial genes and mitochondrial biogenesis. Mol Cell Biol 2005;25:6225–34.

32. Bell EL, Klimova TA, Eisenbart J, et al. The Qo site of the mitochondrial complex III is required for the transduction of hypoxic signaling via reactive oxygen species production. J Cell Biol 2007;177:1029–36.

33. Zhang H, Gao P, Fukuda R, et al. HIF-1 inhibits mitochondrial

biogenesis and cellular respiration in VHL-deficient renal cell carcinoma by repression of C-MYC activity. Cancer Cell 2007;11:407 – 20.

34. Thastrup O, Cullen PJ, Drobak BK, Hanley MR, Dawson AP. Thapsigargin, a tumor promoter, discharges intracellular Ca^{2+} stores by specific inhibition of the endoplasmic reticulum Ca^{2+}-ATPase. Proc Natl Acad Sci U S A 1990;87:2466 – 70.

35. Barsyte-Lovejoy D, Mao DY, Penn LZ. c-Myc represses the proximal promoters of GADD45a and GADD153 by a post-RNA polymerase II recruitment mechanism. Oncogene 2004;23:3481 – 6.

36. Ali H, Maeyama K, Sagi-Eisenberg R, Beaven MA. Antigen and thapsigargin promote influx of Ca^{2+} in rat basophilic RBL-2H3 cells by ostensibly similar mechanisms that allow filling of inositol 1,4,5-trisphosphate-sensitive and mitochondrial Ca^{2+} stores. Biochem J 1994;304:431 – 40.

37. Hoek JB, Farber JL, Thomas AP, Wang X. Calcium ion-dependent signalling and mitochondrial dysfunction: mitochondrial calcium uptake during hormonal stimulation in intact liver cells and its implication for the mitochondrial permeability transition. Biochim Biophys Acta 1995;1271:93 – 102.

38. Beaver JP, Waring P. Thapsigargin induces mitochondrial dysfunction and apoptosis in the mastocytoma P815 cell line and in mouse thymocytes. Cell Death Differ 1996;3:415 – 24.

39. Koshiji M, Kageyama Y, Pete EA, Horikawa I, Barrett JC, Huang LE. HIF-1α induces cell cycle arrest by functionally counteracting Myc. EMBO J 2004;23:1949 – 56.

Molecular Cancer Therapeutics

Mitochondrial regulation by c-Myc and hypoxia-inducible factor-1 α controls sensitivity to econazole

Yongmao Yu, Maryam Niapour, Yicheng Zhang, et al.

Mol Cancer Ther 2008;7:483-491.

Updated version	Access the most recent version of this article at: http://mct.aacrjournals.org/content/7/3/483

Cited articles	This article cites 39 articles, 13 of which you can access for free at: http://mct.aacrjournals.org/content/7/3/483.full#ref-list-1
Citing articles	This article has been cited by 2 HighWire-hosted articles. Access the articles at: http://mct.aacrjournals.org/content/7/3/483.full#related-urls

E-mail alerts	Sign up to receive free email-alerts related to this article or journal.
Reprints and Subscriptions	To order reprints of this article or to subscribe to the journal, contact the AACR Publications Department at pubs@aacr.org.
Permissions	To request permission to re-use all or part of this article, use this link http://mct.aacrjournals.org/content/7/3/483. Click on "Request Permissions" which will take you to the Copyright Clearance Center's (CCC) Rightslink site.